Biomaterials 262 (2020) 120342

Contents lists available at ScienceDirect

Biomaterials

journal homepage: www.elsevier.com/locate/biomaterials

Adaptable antigen matrix platforms for peptide vaccination strategies and T cell-mediated anti-tumor immunity

Sjoerd T.T. Schetters [a,*], R.J. Eveline Li [a], Laura J.W. Kruijssen [a], Steef Engels [a], Martino Ambrosini [a], Juan J. Garcia-Vallejo [a], Hakan Kalay [a], Wendy W.J. Unger [b], Yvette van Kooyk [a,*]

[a] Department of Molecular Cell Biology and Immunology, Amsterdam UMC, Location VUmc, Amsterdam, Netherlands
[b] Laboratory of Pediatrics, Division of Pediatric Infectious Diseases and Immunology, Erasmus MC-Sophia Children's Hospital, Rotterdam, Netherlands

ARTICLE INFO

Keywords:
Vaccination
Adaptive immunity
T cell
Cytotoxic T cell
Antigen presentation
Dendritic cell targeting
MF59
AddaVax
DC-SIGN
Peptide
Adjuvants

ABSTRACT

Injection of antigenic peptides has been widely used as a vaccine strategy to boost T cell immunity. However, the poor immunogenicity of single peptides can potentially be strengthened through modification of the tertiary structure and the selection of the accompanying adjuvant. Here, we generated antigenic peptides into non-linear trimers by solid phase peptide synthesis, thereby enhancing antigen presentation by dendritic cells to $CD8^+$ T cells *in vitro* and *in vivo*. $CD8^+$ T cells from mice vaccinated with trimers showed an $KLRG1^+$ effector phenotype and were able to recognize and kill antigen-expressing tumor cells *ex vivo*. Importantly, trimers outperformed synthetic long peptide in terms of T cell response even when equal number of epitopes were used for immunization. To improve the synthesis of trimers containing difficult peptide sequences, we developed a novel small molecule that functions as conjugation platform for synthetic long peptides. This platform , termed Antigen MAtriX (AMAX) improved yield, purity and solubility of trimers over conventional solid phase synthesis strategies. AMAX outperformed synthetic long peptides in terms of both $CD8^+$ and $CD4^+$ T cell responses and allowed functionalization with DC-SIGN-binding carbohydrates for *in vivo* dendritic cell targeting strategies, boosting T cell responses even further. Moreover, we show that agonistic CD40 antibody combined with MF59 (AddaVax) emulsion synergistically improves the antigen-specific T cell response of the AMAX *in vivo*. Also, tumor-associated antigens and neo-antigens could be incorporated in AMAX for tumor-specific $CD8^+$ T cell responses. Importantly, immunization with a mix of neoantigen AMAX could reduce tumor growth in a pre-clinical syngeneic mouse model. Hence, we provide pre-clinical support for the induction of effector $CD8^+$ T cells through the adaptable AMAX platform as easy implementable peptidic vaccination strategy against any antigen of choice, including neoantigens for anti-tumor immunity.

1. Introduction

T cell-mediated immune responses can protect the host against intracellular pathogens, non-functional cells and transformed cells, like tumor cells. The ability of the immune system to recognize and deal with these host-damaging processes is dependent on antigens presented on MHC class I (MHCI). While the host is generally capable of inducing these antigen-specific responses upon infection, artificial inducers of immunity like vaccines can initiate these responses in absence of damaging pathogens. Tumor- and pathogen-associated antigens in the form of peptides can be used in vaccines to induce antigen-specific immune responses. However, peptidic vaccines are inherently of low immunogenicity and are therefore often coupled to immunogenic carrier proteins like keyhole limpet hemocyanin (KLH) or formaldehyde-inactivated diphtheria toxoid (DT) [1]. Synthetic long peptides can additionally be conjugated to poly-lysine cores into dendrimers with high molecular weight, called multiple peptide antigen systems (MAPs) [2]. Another approach is to chemically synthesize antigens in the form of long peptides and combine these with innate immune stimuli like adjuvants [3]. Using active immunotherapy with carefully determined antigenic peptides ensures both rapid effector phases of immunity as well as the formation of immunological memory needed for prolonged disease-free conditions.

In the era of genomic-based antigen discovery and high throughput

* Corresponding authors.
E-mail addresses: sjoerds@irc.vib-ugent.be (S.T.T. Schetters), y.vankooyk@amsterdamumc.nl (Y. van Kooyk).

https://doi.org/10.1016/j.biomaterials.2020.120342
Received 29 May 2020; Received in revised form 17 August 2020; Accepted 21 August 2020
Available online 28 August 2020

mass spectrometry, the antigens presented by infected or malignant cells are increasingly being identified and exploited for vaccine design [4,5]. For example, by isolating MHCI-bound peptides of glioblastoma tumor tissue and subsequently performing liquid chromatography–mass spectrometry (LC-MS), shared antigens expressed specifically by glioblastoma in tumor patients can be identified [6]. Using these glioblastoma-specific antigens in a therapeutic peptide vaccine has since been used in clinical trials [7,8]. Alternatively, using complementary whole-exome sequencing, transcriptome sequencing analysis and mass spectrometry, immunogenic peptide vaccines can be formulated, capable of generating T cell responses specifically to cancer cells and not healthy tissue [9,10]. Hence, peptide-based vaccine strategies that can induce durable immune responses are increasingly explored. Specificity derived from antigen is not sufficient; an adjuvant is needed to provide adequate immune stimulation in concert with the provided antigen [11]. While current approved adjuvants are successful in inducing protective antibody responses, generating T cell immunity has proven a much more difficult challenge [12]. Our understanding of T cell immune activation has significantly improved over the last decades, including the identification of dendritic cells as initiators of adaptive immune responses and the receptors they employ to recognize foreign particles and mediate immune activation [13]. Therefore, adjuvants aimed at inducing dendritic cell (DC) activation or antigens specifically targeting DCs may improve T cell immunity.

While MHCI molecules needed for the induction of $CD8^+$ T cell responses typically present peptide of 8–10 amino acids long, vaccination with these short peptide has been shown to induce T cell dysfunction at the vaccination-site because of persistent antigen in non-antigen presenting cells [14]. Instead, peptides need to be lengthened to the extent that MHCI loading only occurs in cells capable of internalizing material and presentation of processed peptide on MHCI to T cells, for example dendritic cells [14]. Therefore, synthetic long peptides containing disease-associated antigens have been preferred in vaccination strategies against viral infections [15] and cancer [16,17].

In this study, we show increased T cell immunogenicity of synthesized trimeric peptidic structures compared to single long peptides. To facilitate easy and reproducible synthesis, we design a chemical nanoplatform that facilitates the efficient conjugation of pre-synthesized peptides into trimeric structures termed Antigen MAtriX (AMAX). We show that AMAX combined with the prototypical adjuvant for peptidic vaccines, agonistic CD40, is synergistically enhanced by the clinically approved adjuvants MF59 (AddaVax). We also show that AMAX can be chemically modified with the DC-SIGN carbohydrate ligand, Lewis Y, to facilitate DC targeting to the endocytic receptor DC-SIGN and consequently enhance the T cell-mediated immune response in human DC-SIGN transgenic mice. In a tumor setting, AMAX platform could accommodate several antigens, including neo-antigens, for combination therapy with for antagonistic PD1 antibody therapy. Finally, neo-antigen immunization reduced tumor growth *in vivo*.

2. Material and methods

2.1. Mice

Mice transgenic for hDC-SIGN, OT-I and OT-II on the C57BL/6 background were bred at the animal facility of VU University (Amsterdam, Netherlands) under specific pathogen-free conditions and used at 12–32 weeks of age. Mice transgenic for hDC-SIGN, OT-I and OT-II on the C57BL/6 background have been described previously [18–20]. Female and male mice were equally divided among groups, unless stated otherwise. All experiments were approved by the Animal Experiments Committee of the VU University and performed in accordance with national and international guidelines and regulations.

2.2. Flow cytometry facilities and reagents

All flow cytometry experiments were performed at the O2 Flow Facility at VU University (Amsterdam, Netherlands) using an X20 Fortessa flow cytometer (BD Biosciences) and ImageStreamX (Amnis Corp.) imaging flow cytometer. All antibodies were purchased from Biolegend, Miltenyi and eBioscience (ThermoFisher), specifically: anti-IFNγ (Clone XMG1.2), anti-TNFα (Clone TN3-19), anti-IL2 (Clone JES6-5H4), anti-CD44 (Clone IM7), anti-KLRG1 (Clone 2F1/KLRG1), anti-CD62L (Clone MEL-14), anti-CD4 (Clone GK1.5), anti-CD8 (Clone H35–17.2), anti-CXCR3 (Clone CXCR3-173), anti-CD11b (Clone M1/70), anti-B220 (Clone RA3-6B2), anti-CD45 (Clone 30-F11), anti-CD3 (Clone 145-2C11), anti-MHCII (Clone M5/114.15.2), anti-CD16/32 (Clone 93), Fixable viability dye-eFluor 780 (Thermo Fisher). $OVA_{257\text{-}264}$-H2-Kb-PE and GP100-H2-Kb-PE tetramers were a kind gift from Dr. J.W.Drijfhout at the LUMC, Leiden, Netherlands.

2.3. Chemicals and peptide synthesis

Chemicals were obtained from commercial suppliers and used without further purification. All Fmoc-amino acids and trifluoro acetic acid (TFA) were purchased from Novabiochem. Rink amide Chemmatrix resin, triisopropylsilane (TIS), Ethanedithiol (EDT), Triethylamine (TEA), Dimethylsulfoxide (DMSO) and diethyl ether were purchased from Sigma Aldrich. Piperidine, acetonitrile, N,N-dimethyl formamide (DMF) were purchased from Biosolve. All peptides were synthesized by solid phase peptide synthesis using Fmoc chemistry on a peptide synthesizer (Protein Technologies Inc.) at the GlycO2pep unit. The peptides were purified on a preparative Ultimate 3000 HPLC system (Thermo Fisher) over a Vydac 218MS1022 C18 25 × 250mm column (Grace Davidson). Confirmation of purity and mass was achieved by the Ultimate 3000 UHPLC system (Thermo Fisher) hyphenated with an LCQ-Deca XP Iontrap ESI mass spectrometer (Thermo Finnigan) via a RSLC 120 C18 Acclaim 2.2 μm particle 2.1 × 250 mm column and sample ionization in positive mode.

2.4. Peptide sequences

OTI-OTII sequence: EEKSIINFEKLISQAVHAAHAEINEAGRKEEK, GP100-PADRE sequence: EEKKVPRNQDWLAKFVAAWTLKAAAKEEK, TRP1-TRP2 sequence: EEKCRPGWRGAACNQKISVYDFFVWLKEEK, MC38 neoantigen sequences Dpagt1-OTII: EEKSIIVFNLLISQAVHAA-HAEINEAGRKEEK; Reps1-OTII: EEKAQLANDVVLISQAVHAAHAEI-NEAGRKEEK; Adpgk-OTII: EEKASMTNMELMISQAVHAAHAE INEAGRKEEK; OTI-OTIII: EEKSIINFEKLEKLTEWTSSNVMEERKEEK

2.5. Single chain synthetic long peptide and trimer

The single chain synthetic long antigen peptides were synthesized completely on solid phase. After the synthesis of first arm, Fmoc-Lys (Fmoc)-OH was added to the peptidic chain to achieve branching. The synthesis proceeded simultaneously on both α and ε amino groups of "the core-lysine" to synthesize the second and third arm. The peptides were cleaved from the resin using a cleavage solution containing 92.5% TFA, 2.5% MilliQ, 2.5% TIS and 2,5% EDT. The peptides were collected, lyophilized and purified by HPLC.

2.6. Single branched trimeric long peptidic conjugates; the Antigen Matrix (AMAX)

To synthesize the AMAX-core 1 equivalent of Tris (2-aminoethyl) amine (5.45 mg, 37 μmoles) reacted with 3.2 equivalents of LC-SMCC ((succinimidyl 4-(N-maleimidomethyl)cyclohexane-1-carboxy-(6-amidocaproate), Thermo Scientific) (50 mg, 118 μmoles) in anhydrous DMSO. The reaction was incubated for 1 h at room temperature and purified over prepHPLC. The AMAX conjugates were generated by

conjugation of single arm peptides containing a C-terminal cysteine with the AMAX-core. Briefly, 4 equivalents of single arm peptide were added to AMAX-core in DMSO containing 50–100 mM TEA. After incubation for 1 h at room temperature the conjugates were purified over PrepHPLC and analyzed over mass spectometry.

2.7. Murine bone marrow-derived and splenic CD11c$^+$ dendritic cells

Bone marrow-derived dendritic cells were cultured as described by Lutz et al. [21]. Splenic CD11c$^+$ dendritic cells were isolated using a combination of enzymatic digestion and MACS sorting using the CD11c-magnetic isolation kit. In short, mice were sacrificed and the spleen isolated and cut small using sterile scissors in 385 μg/ml liberase TL (2WU) and incubated at 37 °C for 20 min. Enzymes were deactivated using ice-cold RPMI 1640 complete (10% FCS, 1% 50 U/mL penicillin, 50 μg/ml streptomycin, HEPES/EDTA). After digestion, cells were run through a 100 μm cell strainer and extensively washed before MACS sorting. Splenic CD11c$^+$ dendritic cells were isolated using a CD11c-magnetic isolation kit according to manufacturer's instructions (MagniSort™, eBioscience/ThermoFisher). Purity of CD11c$^+$ cells was typically >96% of alive cells.

2.8. Imaging flow cytometry and sample preparation (tumor cell killing assay)

Spleens were harvested from vaccinated mice after prime-boost injections with the reported product. Spleens were mechanistically disrupted and filtered through a 70 μm cell strainer. Red blood cells were lysed using ACK lysis buffer (0.15 M NH_4Cl, 10 mM $KHCO_3$, 0.1 mM EDTA), washed and counted before purification using MagniSort Mouse CD8-negative isolation kits according to manufacturer's instructions (eBioscience/Thermo Fisher). Equal number of splenocytes from mice within a group were pooled before purification. After purification (typically >95% of alive cells), CD8$^+$ T cells were co-cultured with CFSE-labeled OVA-expressing GL26 glioblastoma cells for 18 h in a tumor/T cell ratio of 1:10, respectively. After co-culture, supernatant was harvested for interferon γ cytokine detection and the total cell culture was used for further imaging flow cytometry analysis. Next, the cells were stained with anti-CD8, Hoechst and fixable viability dye for 30 min at 4 °C. Cells were washed with PBS twice and fixed for 15 min using ice-cold 4% PFA. After washing twice, the fixed cells were resuspended in PBS. Cells were analyzed on the ImageStream X100 (Amnis-Merck Millipore) imaging flow cytometer as previously described (22). A minimum of 15,000 cells were acquired per sample. Analysis was performed with single cells after compensation (with a minimum of 5000 cells).

2.9. FACS acquisition and analyses

All samples were acquired on an X20 Fortessa flow cytometer (BD Biosciences), of which the performance was checked and calibrated daily with CS&T beads (BD Biosciences). Detector voltage settings were set initially based on daily CS&T settings and only adjusted when fluorescent signal was off-scale, with a maximum adjustment of 100 values. Aqcuisition of samples was done using the high throughput sampler (HTS), measuring samples at a max of 2.0 μL/second at an acquisition rate <15.000 events/second. After acquisition, samples were compensated using fluorescently labeled beads and adjusted according to FMO experimental samples acquired within the same experiment. Gating strategies were based on a combination of FMO and expert gating knowledge. For tSNE unsupervised clustering analysis, compensated populations were concatenated and exported as FCS files per experimental group using FlowJo 10 software and uploaded to the Cytobank online cloud-based flow cytometry platform (https://www.cytobank.org/). For the tSNE analysis in Fig. 2 an equal number of 4770 antigen-specific CD8$^+$ T cells from peptide and trimer conditions was used for input (9540 total). Clustering was performed based on expression of KLRG1, CD127, CD62L and CD44 for 2000 iterations and a theta of 50. For the tSNE analysis in Fig. 7 an equal number 12049 antigen-specific CD8$^+$ cells of each condition was used for input (36,147 in total). Since all antigen-specific CD8$^+$ T cells from these conditions were CD44$^+$CD62L$^-$, the expression of CD127, KLRG1 and CXCR3 for 2000 iterations and a theta of 50 was used to cluster subpopulations. Data and statistics presented in bar graphs are expertly gated in FlowJo based on tSNE-aided gating strategies using all individual samples per experimental groups.

2.10. Cytokine ELISA

The cytokine IFNγ was determined in supernatant of tumor/T cell cocultures using a commercially available ELISA kit and performed according to the manufacturer's instructions (eBioscience 5017319). In short, NUNC ELISA plates were coated using IFNγ capture antibody in 1x coating buffer O/N. Wells were blocked using 1x ELISA diluent. Samples were incubated at RT for 2 h. Detection antibody was diluted in ELISA diluent and incubated for 1 h at RT. Avidin-HRP diluted in ELISA diluent was added to the wells and incubated for 30 min on RT. TMB solution was added till the standard was stained. The ELISA was stopped using 2 N H2SO4. The plate was measured on a BioRad iMark microplate reader at 450 nm.

2.11. Antigen presentation assays

OTI and OTII transgenic mice were sacrificed and spleens were mechanistically disrupted and filtered through a 70 μm cell strainer. Red blood cells were lysed using ACK lysis buffer (0.15 M NH_4Cl, 10 mM $KHCO_3$, 0.1 mM EDTA) and washed before purification using MagniSort Mouse CD4$^-$ or CD8-negative isolation kits according to manufacturer's instructions (eBioscience/Thermo Fisher). Purified CD4$^+$ and CD8$^+$ T cells were labeled using 2 μM CFSE and counted before co-culture. BMDCs were pulsed with product at indicated concentrations in the presence of medium, 2 μg/ml MPLA or 2 μg/ml Poly I:C for 3 h. After extensive washing of the BMDCs, purified T cells were co-cultured for 3 days at 37 °C, stained and measured on an X-20 Fortessa flow cytometer. Proliferation results are calculated and represented as percentage responding T cells ('calculated cells at the start of culture'/'number of cells that went into division'*100).

2.12. Vaccination

Mice were subcutaneously vaccinated with synthetic long peptides, trimers or AMAX mixed with 25 μg of anti-CD40 in 1:1 PBS/AddaVax emulsion according to manufacturer's instructions (InvivoGen) in a maximum volume of 100 μL. Synthetic long peptides were injected at a mass of 15 nmol and trimers or AMAX were injected at a mass of 5 nmol per mouse per injection.

2.13. Isolation and analysis of leukocytes from the blood and spleen of vaccinated mice

Mice were bled by cheek-pinch and approximately 100 μL of blood was collected in heparin-coated tubes. Red blood cells were lysed using ACK lysis buffer (0.15 M NH_4Cl, 10 mM $KHCO_3$, 0.1 mM EDTA) and washed before staining. Mice were sacrificed and spleens were mechanistically disrupted and filtered through a 70 μm cell strainer. Red blood cells were lysed using ACK lysis buffer and washed before counting and subsequent staining protocols. Single cells suspensions from spleens and blood of vaccinated mice were incubated with $OVA_{257-264}$-H2-Kb-PE or GP100-H2-Kb-PE tetramers together with CD8a PerCP for 45 min at room temperature. Cell were washed and incubated with other directly labeled primary antibodies before mild fixation with 2% PFA for 15 min at 4 °C.

2.14. Ex vivo peptide restimulation and intracellular cytokine detection

Single cell suspensions of spleens were counted and 3×10^6 cells were restimulated with short peptide for either 6 h ($CD8^+$ T cell restimulation) or 48 h ($CD4^+$ T cell restimulation) in the presence of 10 μg/ml or 100 μg/ml cognate antigen (short peptide), respectively. The last 6 h of the restimulation was in the presence of 1 μg/ml Brefeldin A. Cells were harvested and first stained for CD8b or CD4 and fixable viability dye. Next, the stained cells were washed with PBS and fixed with 4% PFA in PBS for 15 min at 4 °C. After fixation, the cells were permeabilized with 0,5% saponin in PBS/BSA 0,5% buffer for 15 min. Intracellular cytokines were subsequently stained with anti-IFNγ and anti-TNFα for 30 min at room temperature in 0,5% saponin PBS/BSA 0,5% buffer. Finally, cell suspensions were acquired and analyzed using flow cytometry.

2.15. In vivo anti-tumor immunization

Mouse MC38 colorectal carcinoma tumor cells were cultured in DMEM up to 90% confluency in T75/T175 flasks before injection. Mice were anesthetized using 2% isoflurane, flanks were shaved and tumor cells in serum-free medium were subcutaneously injected in a volume of 50 μL. Tumor size was measured using digital calipers every two days in a double-blind manner. Total tumor volume was calculated using formula $4/3 \times \pi \times abc$ (a = width of the tumor/2, b = length/2 and c = the average of a and b). Mice were sacrificed when tumor exceeded 800 mm3 or at the end of the study (day 23). Subcutaneous immunization in the neck was performed at day 7 after tumor cell injection, whereas treatment using antagonistic PD1 antibody (clone RMP1-14, in house, endotoxin free) was started at day 9 after tumor cell injection.

2.16. Statistics

Statistics were performed using GraphPad Prism 6 software. For the comparison of two groups a student's *t*-test was used. For more than two groups a two-way analysis-of-variance (ANOVA) was used followed by a Tukey posthoc analysis to compare means between two groups. *P < 0.05, **P < 0.01, ***P < 0.001, ***P < 0.0001, data represented as mean + −SEM.

3. Results

3.1. Solid phase allows synthesis of antigenic long peptides and multivalent trimers for antigen presentation by dendritic cells

Peptides are widely used in vaccination strategies to boost antigen-specific immunity. With efficient induction of T cell specific responses in clinical trials, in addition to low vaccine toxicity and high patient tolerance, these synthetic long peptides are fundamental components in immunotherapeutic strategies [22]. The synthesis of long peptides for the use of antigenic vaccine compounds is typically performed using liquid or solid phase synthesis using fluorenylmethyloxycarbonyl protecting group (Fmoc) chemistry. To study whether multivalent representation of synthetic peptides would improve immune responses, we used this method to prepare single chain synthetic long peptides and single branched trimeric long peptide. The synthesis of the single chain synthetic long peptide is achieved via successive reactions of amino acid derivatives of the first peptide arm on resin. The synthesis of single branched trimeric long peptide involves the further elongation using lysine with an α and ε amino group. The two amino groups on the core lysine allows parallel extension of the peptide into a second and third branch, resulting in the formation of a peptidic trimer (Fig. 1A). We started off making use of OVA peptides as model antigens to compare

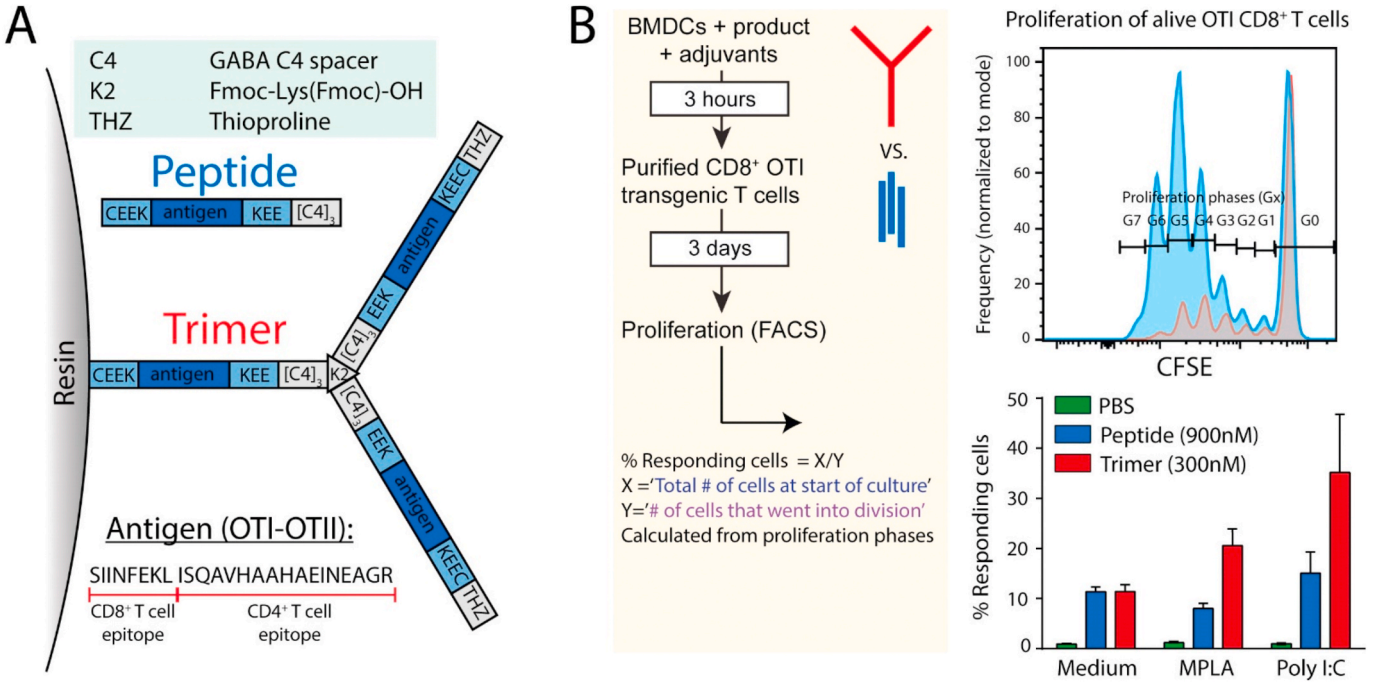

Fig. 1. | Solid phase synthesis of linear long peptides and trimers produces products that can be processed and presented by (bone marrow-derived) dendritic cells to $CD8^+$ T cells *in vitro*. A. Long peptides were synthesized using solid phase peptide synthesis. Additionally, using a lysine with an α and ε amino group after the first peptide, the molecule is extended with a second and third branch simultaneously. This results in a trimer containing three peptides. **B.** Bone marrow-derived dendritic cells (BMDCs) were incubated with either 900 nM peptide or 300 nM trimer in the presence or absence of 2 μg/ml monophosphoryl lipid A (MPLA) or 10 μg/ml polyinosinic:polycytidylic acid (Poly I:C) for 3 h. After washing away the product and adjuvants, BMDCs were incubated with freshly purified CFSE-labeled $CD8^+$ T cells from OTI transgenic mice for 3 days. Cultures were harvested and proliferation of $CD8^+$ T cells was measured by dilution of CFSE. The percentage of OTI $CD8^+$ T cells that result in proliferation is increased by peptide and antigen matrix in an antigen-specific manner. Data (mean ± SEM of biological triplicate) is representative of 2 independent experiments.

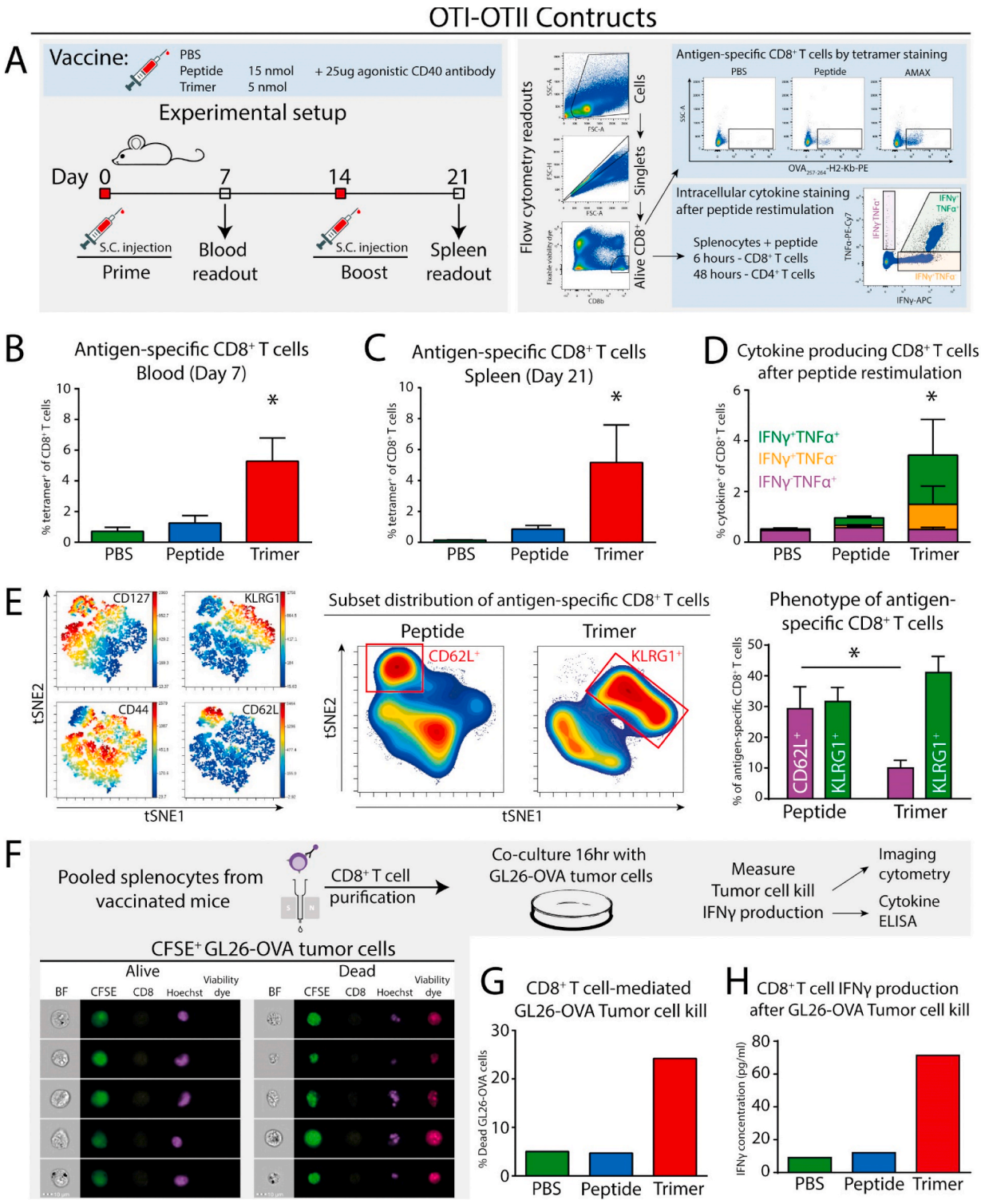

Fig. 2. | Trimers induce potent CD8$^+$ T cell responses with an effector phenotype and tumor cell killing capacity. A. Mice were subcutaneously vaccinated on day 0 (prime) and on day 14 (boost) with PBS, 15 nmol peptide or 5 nmol trimer with 25 μg agonistic CD40 antibody. Blood was collected on day 7 and spleen was collected after sacrificing the animals on day 21. **B.** A single dose of trimer induces significantly higher numbers of antigen-specific CD8$^+$ T cells. **C.** 7 days after the boost vaccination, the trimer still outperformed the peptidic form of the vaccine formulation. **D.** CD8$^+$ isolated from trimer-vaccinated mice showed polyfunctionality as demonstrated by the significantly higher number of single (IFNγ$^+$) and double (IFNγ$^+$TNFα$^+$) producing CD8$^+$ T cells after peptide re-stimulation. **E.** tSNE unsupervised clustering analysis of antigen-specific CD8$^+$ T cells identifies heterogeneity based on CD62L, CD44, KLRG1 and CD127 (expression as color code). The phenotype of isolated CD8$^+$ T cells from trimer-vaccinated mice is characterized by increased effector differentiation (CD62L$^-$ and KLRG1$^+$). **F.** CD8$^+$ T cells purified from splenocytes from vaccinated mice were pooled per group and cultured for 16 h with ovalbumin-expressing GL26 tumor cells. **G.** Purified CD8$^+$ T cells from trimer-vaccinated mice showed increased tumor killing capability compared to CD8$^+$ T cells from peptide-vaccinated mice as measured by imaging flow cytometry. **H.** Additionally, IFNγ production was increased after 16 h of T cell/tumor cell co-culture. Data (mean ± SEM) is representative of 2 independent experiments with group size N = 5/6. Statistics by one-way ANOVA with Tukey post-hoc multiple comparison test; *$p < 0.05$. (For interpretation of the references to color in this figure legend, the reader is referred to the Web version of this article.)

their efficacy in single and multivalent representation.

Synthetic long peptides incorporating multiple antigens and flanking regions need to be enzymatically processed inside the cell for loading to MHC class I and –II complexes and presentation to T cells. To test whether the synthesized constructs are adequately processed and presented to T cells in an antigen-specific manner, we performed antigen presentation experiments *in vitro*. We generated bone marrow-derived dendritic cells (BMDCs), as previously described [21]. BMDCs were pulsed with peptide or trimer in concentrations with equal antigenic epitopes for 3 h. Co-culture with antigen-specific OTI $CD8^+$ T cells showed efficient internalization, processing and presentation to $CD8^+$ T cells (Fig. 1B). Interestingly, in conditions of increased adjuvanticity (with MPLA/Poly I:C) BMDCs pulsed with trimers outperformed those loaded with the synthetic long peptides (Fig. 1B).

3.2. Multivalent trimeric constructs increase $CD8^+$ T cell immunity compared to single long peptides

Having established the correct peptidic and trimeric structures for antigen presentation *in vitro*, we investigated the potency of these products to elicit *de novo* immune responses in a vaccination setting *in vivo*. The potency of the vaccine was tested in a typical prime-boost vaccination strategy including agonistic CD40 antibody as adjuvant (Fig. 2A). Seven days after the prime injection blood was isolated and the percentage of antigen-specific $CD8^+$ T cells was measured by flow cytometry. Using a SIINFEKL-H2-kb tetramer, we found that trimers induced higher numbers of antigen-specific $CD8^+$ T cells, compared to the synthetic long peptide (Fig. 2B). The vaccinated mice were then sacrificed 7 days after the second boost vaccination and the number and function of $CD8^+$ T cells was investigated. Similar to blood-derived lymphocytes after the prime vaccination, antigen-specific $CD8^+$ T cell numbers were significantly higher in number in mice vaccinated with trimers compared to the synthetic long peptides (Fig. 2C). Furthermore, by re-stimulation with short peptide and intracellular cytokine staining, a significantly higher number of $CD8^+$ T cells producing the effector cytokines TNFα and/or IFNγ was detected in mice vaccinated with trimers (Fig. 2D). To show that the gain efficacy of the trimer is not due to its specific antigenic sequence, we generated peptides and trimers containing an alternative $CD4^+$ T cell epitope and show that the trimer of this product also outperforms single peptides (Supplementary Figure 1). Next, we employed an unbiased tSNE unsupervised clustering analysis of the phenotype of antigen-specific $CD8^+$ T cells from vaccinated mice. Using the expression of CD62L, CD44, CD127 and KLRG1 to cluster the antigen-specific $CD8^+$ T cells into subsets (Fig. 2E). Interestingly, antigen-specific $CD8^+$ T cells isolated from the spleen after trimer prime-boost vaccination showed a higher frequency of antigen-specific $CD8^+$ T cells with an effector phenotype, as evidenced by the combined loss of CD62L and gain of KLRG1 expression (Fig. 2E). This suggests not only a quantitative increase in number, but also a qualitative difference between single and trimer peptidic vaccination. Finally, we investigated whether $CD8^+$ T cells from vaccinated mice were able to recognize and kill tumor cells expressing the antigen. We purified $CD8^+$ T cells from either peptide- or trimer-vaccinated mice using negative selection by magnetic isolation and co-cultured these cells with GL26 tumor cells expressing ovalbumin (Fig. 2F). After 16hr of co-culture, we harvested the tumor cells and measured cell death using imaging flow cytometry. Antigen-expressing GL26 tumor cells were more efficiently killed by $CD8^+$ T cells isolated from trimer vaccinated mice, compared to peptide vaccinated mice (Fig. 2G). These data were additionally reproduced using regular flow cytometry (data not shown). In parallel, the supernatant of the tumor cell/$CD8^+$ T cell co-culture from trimer-vaccinated mice contained high amounts of the T cell effector cytokine IFNγ (Fig. 2H), suggesting that $CD8^+$ T cells isolated from trimer vaccinated mice can recognize and kill GL26 tumor cells.

3.3. The antigenic MAtriX (AMAX) core allows the generation of pre-synthesized peptides into AMAX trimers

Next, we aimed to synthesize trimers containing other antigenic epitopes, including the melanoma antigen GP100, which is more challenging than OVA, due to its lower solubility. However, solid phase synthesis depends on the continued elongation of single amino acids to a growing peptide chain. As a result, some amino acid sequences are less efficiently coupled or reduce peptide solubility, further reducing yield and purity of the product. Due to incomplete addition in each reaction, the purity decreases exponentially with the elongation of every amino acid. Considering the length of the single branched trimeric long peptide chain, a low purity can be expected [23]. This is evidenced by the HPLC fractionation and subsequent mass spectrometry of trimers containing GP100 epitopes, but also holds for the peptide chains with the OTIOTII epitopes (Fig. 3A). To circumvent low purity, we designed a nanoplatform that enables conjugation of pre-purified synthetic long peptides into a multivalent conjugate. This trimeric structure remains soluble, increases purity and yield during synthesis without compromising the tertiary structure from trimeric structures. Key to this peptidic conjugate is the core. By reacting a Tris (2-aminoethyl)amine with three equivalents of LC-SMCC, a flexible core was constructed achieving multivalent presentation of single long peptides upon conjugation (Fig. 3B). This results in a highly stable conjugation platform for efficient synthesis of a trimeric peptidic structure we have termed **A**ntigenic **MA**tri**X** (AMAX; Fig. 3B). This synthesis significantly aids HPLC purification and increases yield, while deriving a cleaner product for both the OTIOTII and the GP100 conjugates (Fig. 3C).

3.4. AMAX induces $CD8^+$ and $CD4^+$ T cell activation in vivo, outperforming single peptides

First, to assess the functionality of the synthesized AMAX product, we tested antigen presentation by $CD11c^+$ splenic dendritic cells (Fig. 4A). Splenic DCs pulsed with peptide or AMAX both induced the proliferation of antigen-specific $CD8^+$ T cells (Fig. 4B) and $CD4^+$ T cells (Fig. 4C). Peptide-pulsed splenic DCs were slightly better at inducing $CD4^+$ T cell proliferation compared to AMAX. Addition of innate stimuli like Poly I:C or MPLA in the pulsing phase did not affect antigen presentation to either $CD8^+$ T cells or $CD4^+$ T cells in these conditions (Fig. 4B/C). To test the efficacy of AMAX to generate $CD8^+$ T cell responses *in vivo*, we vaccinated mice with either peptides or AMAX containing similar amounts of antigenic epitopes (Fig. 4D). Seven days after a single dose of AMAX with agonistic CD40 antibody, we detected a significant increase in antigen-specific $CD8^+$ T cells in blood (Fig. 4E). A boost vaccination, 14 days after the prime injection, resulted in similar increased efficacy of AMAX inducing antigen-specific $CD8^+$ T cell responses in the spleen, outperforming single peptides (Fig. 4F). Re-stimulation of splenocytes derived from vaccinated mice with the cognate peptide and intracellular cytokine measurements revealed significant increases of polyfunctional $CD8^+$ T cells producing the effector cytokines IFNγ, TNFα and IL2 (Fig. 4G). Because the synthetic long peptides and AMAX were both able to induce $CD4^+$ T cell proliferation *in vitro*, we additionally investigated the induction of antigen-specific $CD4^+$ T cells by peptide re-stimulation and intracellular cytokine staining. While not statistically significant, AMAX induce higher levels of antigen-specific $CD4^+$ T cells compared to single peptides (Fig. 4H).

3.5. The MF59 (AddaVax) adjuvant synergistically boosts AMAX/αCD40 vaccine efficacy

Even though agonistic CD40 has previously been shown to boost $CD8^+$ T cell responses as adjuvant in peptidic vaccines [24,25], we sought to investigate whether agonistic CD40 antibody could be replaced or combined with the widely used adjuvant MF59 (commercially available as AddaVax). As such, we vaccinated mice with either a

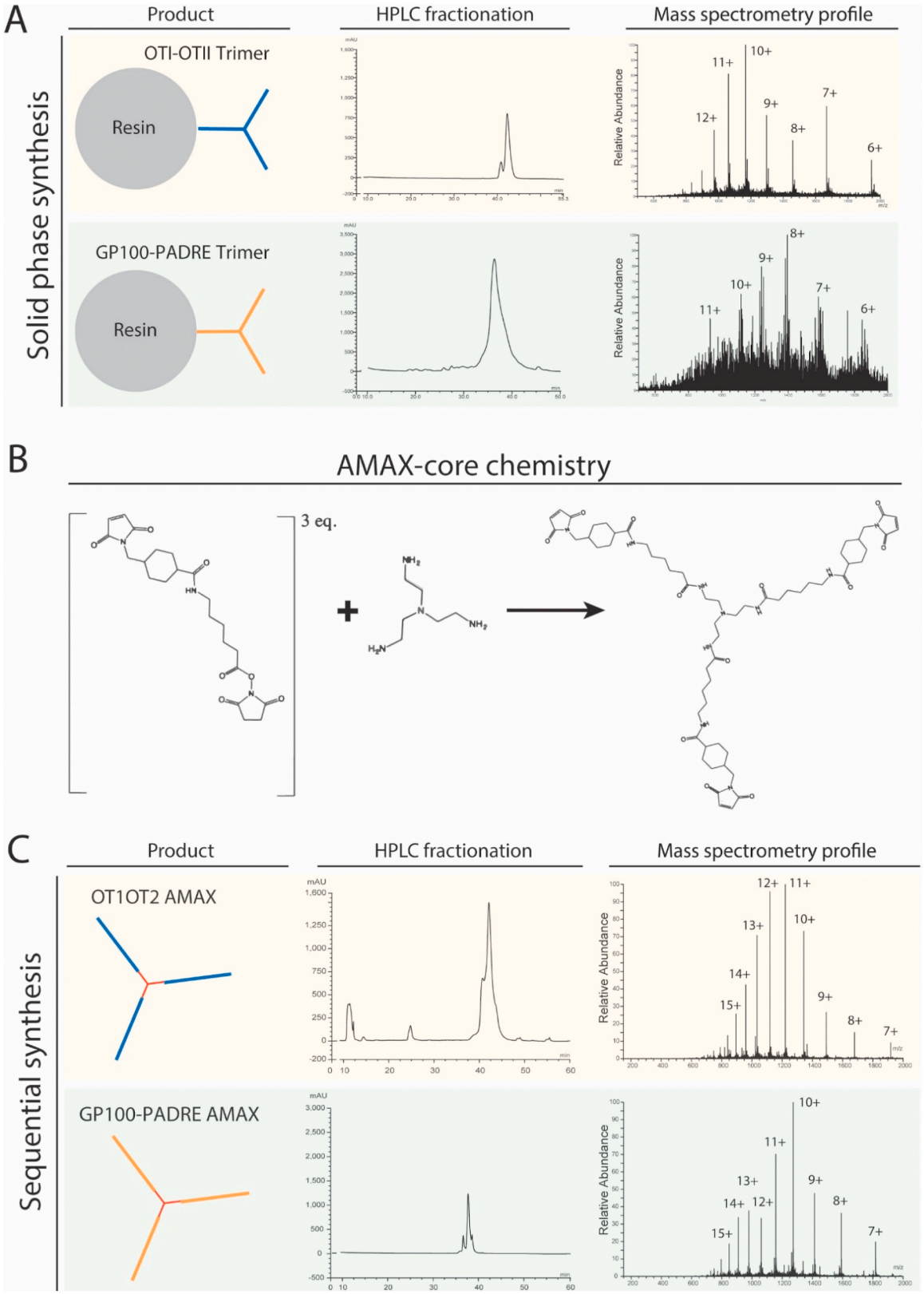

Fig. 3. | Chemical nanoplatform facilitates highly efficient conjugation of pre-synthesized peptides into an Antigenic MAtriX (AMAX) with increased purity, yield and solubility A. Solid phase synthesis inherently hampers the construction of trimers and reduces purity, yield and solubility. HPLC fractionation and mass spectrometry profiles reveal that solid phase synthesis of difficult to synthesize peptides result in poor purity and therefore low yield. **B.** A chemical nanoplatform for conjugation of pre-synthesized long peptides can be made by reacting a Tris (2-aminoethyl)amine with three equivalents of LC-SMCC. **C.** Subsequent conjugation of pre-purified synthetic long peptide to the nanoplatform results in an antigenic matrix (AMAX) with increased purity and yield. Data shown are representative of at least three individual batches of synthesized product.

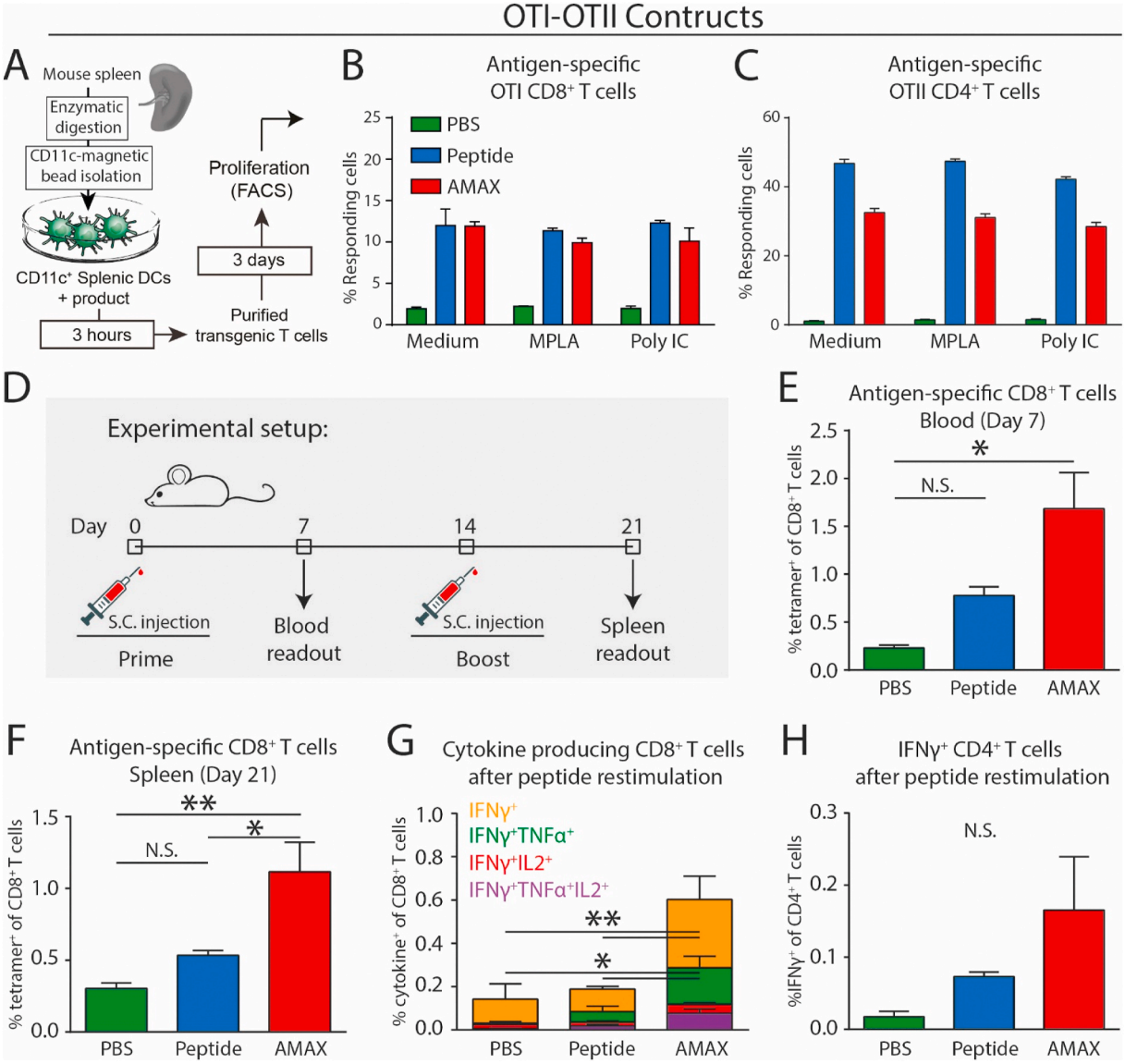

Fig. 4. | AMAX induces potent CD8$^+$ T cell responses *in vitro* and *in vivo* A. Splenic CD11c$^+$ DC were MACS sorted from enzymatically digested spleens and pulsed with 900 nM long peptide or 300 nM AMAX in the presence of medium, 2 μg/ml MPLA or 10 μg/ml Poly I:C for 3 h. After washing away the product and adjuvants, BMDCs were incubated for 3 days with freshly purified CFSE-labeled CD8$^+$ or CD4$^+$ T cells from OTI or OTII transgenic mice, respectively. Proliferation of responding T cells was assessed by flow cytometry **B.** Both peptide and AMAX products were able to induce proliferation of antigen-specific CD8$^+$ T cells by splenic DCs. The adjuvants did not affect the % of responding CD8$^+$ T cells in this setting. **C.** Proliferation of antigen-specific CD4$^+$ was induced by both peptide and AMAX products, although peptide **D.** Mice were subcutaneously vaccinated on day 0 (prime) and on day 14 (boost) with PBS, 15 nmol peptide or 5 nmol AMAX with 25 μg agonistic CD40 antibody. Blood was collected on day 7 and spleen was collected after sacrificing the animals on day 21. **E.** 7 days after the first vaccination antigen-specific CD8$^+$ T cells are significantly higher in the AMAX-vaccinated group. **F.** After the boost, AMAX-vaccinated mice still show significantly increased antigen-specific CD8$^+$ T cells. **G.** CD8$^+$ T cells from AMAX-vaccinated mice are polyfunctional as evidenced by the single (IFNγ$^+$) and double (IFNγ$^+$TNFα$^+$) cytokine production after peptide re-stimulation. **H.** Although not statistically significant, AMAX induce higher levels of antigen-specific CD4$^+$ T cells compared to single peptides. Data (mean ± SEM) is representative of at least two independent experiments with group size N = 9/10. Statistics by one-way ANOVA with Tukey post-hoc multiple comparison test; *p < 0.05 **p < 0.01.

single injection of AMAX with agonistic CD40, AddaVax or the combination of both. Seven days after a single injection, re-stimulation of splenocytes by either CD8 or CD4 reactive peptides, revealed induction of both CD8$^+$ T cells and CD4$^+$ T cells (Fig. 5A and B, respectively). While agonistic CD40 increased the levels of antigen specific CD8$^+$ and CD4$^+$ T cells (as previously shown), AddaVax only induces moderate levels of antigen-specific CD4$^+$ T cells, without induction of antigen-specific CD8$^+$ T cells. Surprisingly, AddaVax combined with agonistic CD40 boosts AMAX-induced antigen-specific CD8$^+$ and CD4$^+$ T cells in a synergistic manner (Fig. 5A–B). Having established the potency of combined adjuvancy of agonistic CD40 antibody in combination with AddaVax, we investigated whether AMAX still outperforms single peptides in a classical prime-boost vaccination scheme (Fig. 5C). Indeed, after a prime-boost vaccination strategy AMAX combined with agonistic CD40 and AddaVax outperforms synthetic long peptides in terms of antigen-specific CD8$^+$ T cells (Fig. 5D). Peptide re-stimulation of splenocytes and intracellular cytokine staining shows similar induction of significantly higher number of CD8$^+$ T cells producing effector cytokines IFNγ and TNFα. (Fig. 5E). While not significant, peptide re-stimulation shows slightly higher numbers of cytokine-producing CD4$^+$ T cells in the AMAX immunized group (Fig. 5F).

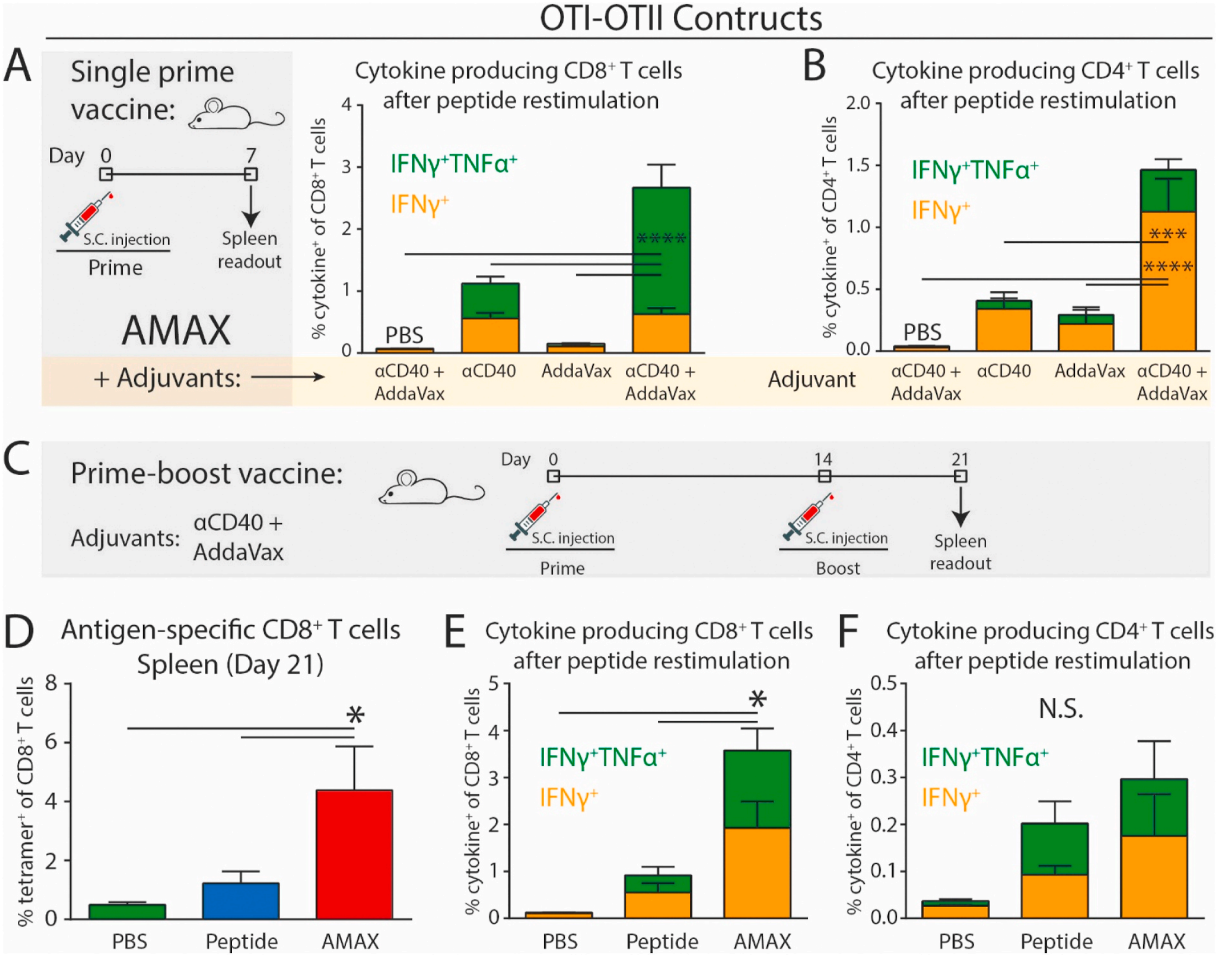

Fig. 5. | AMAX with the adjuvant MF59 (AddaVax) synergistically boosts agonistic CD40 antibody adjuvanticity A. Vaccinating mice with a single dose of AMAX with either agonistic CD40 antibody or AddaVax or the combination affects the induction of antigen-specific $CD8^+$ T cells. Combining the adjuvants synergistically boosts the $CD8^+$ T cell response, with significantly higher amounts of double-producing ($IFN\gamma^+TNF\alpha^+$) $CD8^+$ T cells after peptide re-stimulation. **B.** The combination of agonistic CD40 and AddaVax induces the highest level of antigen-specific $CD4^+$ T cells. **C.** After establishing the best combination of adjuvants, a prime-boost vaccination strategy with agonistic CD40 and AddaVax was performed. **D.** This revealed AMAX as superior in inducing antigen-specific $CD8^+$ T cells compared to single peptides as measured by tetramer staining. **E.** Re-stimulation with peptides and intracellular cytokine staining shows that antigen-specific $CD8^+$ and $CD4^+$ T cells (**F.**) are enriched in AMAX-vaccinated mice. Data (mean ± SEM) is representative of at least two independent experiments with group size N = 9/10. Statistics by one-way ANOVA with Tukey post-hoc multiple comparison test, A,B,E,F statistics on total %cytokine-producing cells; *$p < 0.05$ **$p < 0.01$ ***$p < 0.001$ ****$p < 0.0001$.

3.6. Functionalizing the AMAX platform with the DC-SIGN ligand Lewis Y targets dendritic cells for increased T cell responses

Next, dendritic cells are critical drivers of adaptive immune responses and have therefore been explored as targets for vaccination [26]. Therefore, we explored the AMAX platform as a vector delivery platform to target dendritic cells. More specifically, by chemically conjugating the carbohydrate Lewis Y to the terminal peptidic arms of the AMAX, the resulting AMAX:Lewis Y is hypothesized to bind the dendritic cell-specific C-type lectin receptor DC-SIGN (Fig. 6A) [27], and facilitate processing and presentation of AMAX-including antigens. Using ELISA, we successfully verified intact Lewis Y on the AMAX platform and confirmed the capacity of human DC-SIGN to bind AMAX:Lewis Y using recombinant hDC-SIGN Fc (Fig. 6B). Consequently, to investigate the effect of targeting DC-SIGN expressed by dendritic cells *in vivo*, we vaccinated transgenic mice that express human DC-SIGN (hDC-SIGN) driven by the CD11c-promoter. As a result, dendritic cells specifically express human DC-SIGN in these mice [18]. Vaccination using AMAX:Lewis Y with only agonistic CD40 antibody resulted in increased frequencies of antigen-specific $CD8^+$ T cells compared to unmodified AMAX in two independent experiments (Fig. 6C). After prime-boost vaccination, splenocytes from vaccinated mice were restimulated with short peptide and intracellular cytokine production was measured. A higher frequency of cytokine-producing $CD8^+$ and $CD4^+$ T cells was observed when AMAX was functionalized with the DC-SIGN binding ligand, Lewis Y (Fig. 6D). To test whether AddaVax retained the synergistic augmentation of αCD40 in this setting, we primed mice with one injection of AMAX:Lewis Y/αCD40 with either PBS, the TLR4-activator monophosphoryl lipid A (MPLA) or AddaVax (Fig. 6E). The frequency of antigen-specific $CD8^+$ T cells was highly increased when AddaVax was used, compared to αCD40 alone or even in combination with MPLA (Fig. 6E). Peptide restimulation of splenocytes from vaccinated mice showed that the synergistic effect of AddaVax was most pronounced in the $CD8^+$ T cell compartment in this setting (Fig. 6F). To further investigate the effect of AddaVax on the phenotype of antigen-specific $CD8^+$ T cells, we used tSNE unsupervised clustering. Since all antigen-specific $CD8^+$ T cells in these conditions were $CD62L^-CD44^+$, we used CD127, KLRG1 and CXCR3 to cluster (Fig. 6G). AddaVax-adjuvanted AMAX:Lewis Y/αCD40 vaccine combinations showed significant enrichment of antigen-specific $KLRG1^+$ terminally differentiated effector $CD8^+$ T cells (Fig. 6H). Hence, by targeting the AMAX directly to DC-SIGN on dendritic cells *in vivo*, an even more

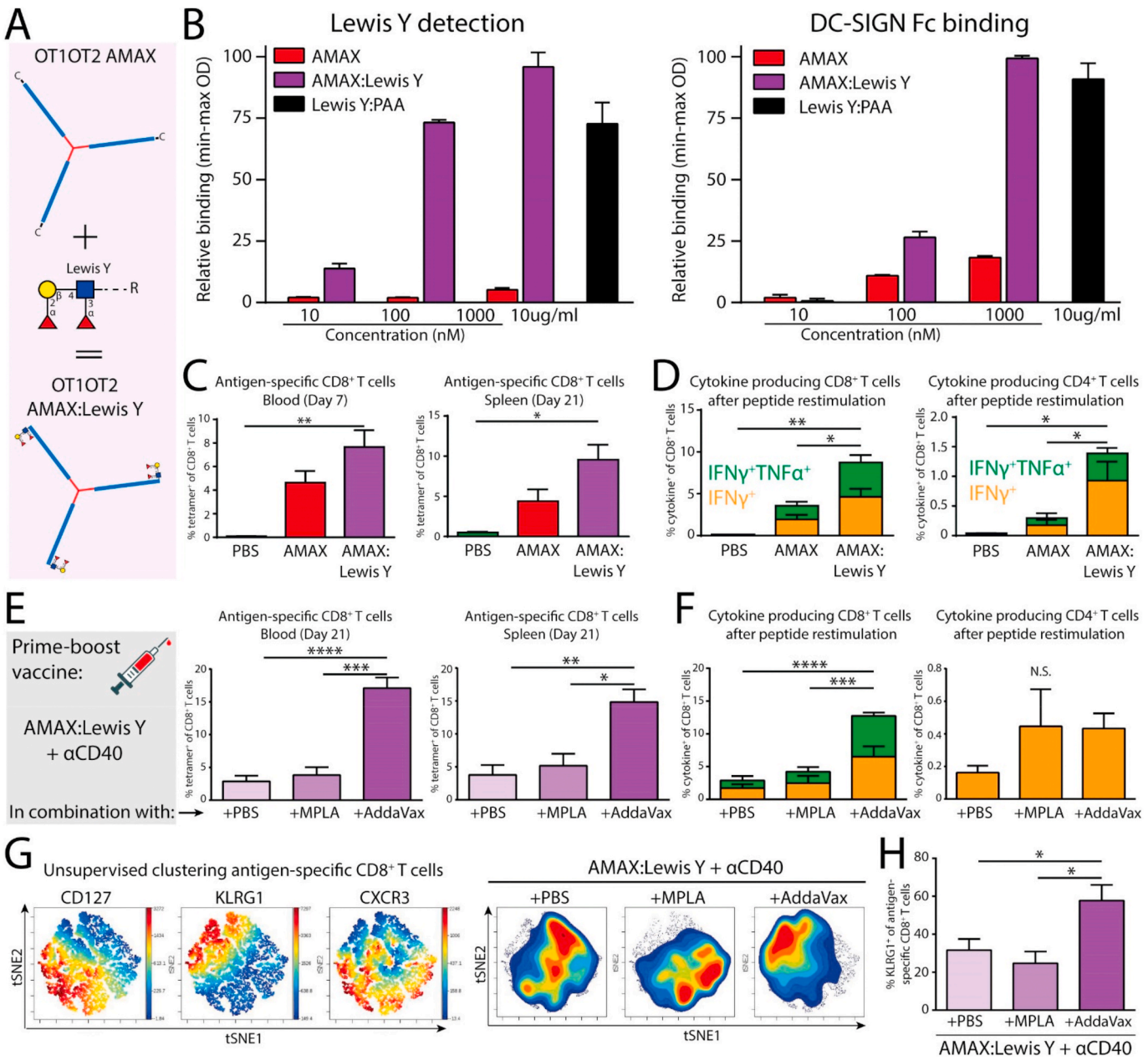

Fig. 6. | AMAX modified with DC-targeting ligands can further improve antigen delivery and adaptive immune responses during prime-boost vaccination strategies A. OTI-OTII AMAX constructs can be chemically modified with the DC-SIGN carbohydrate ligand, Lewis Y. B. The presence of intact Lewis Y was verified by ELISA, as well as the capacity to bind human DC-SIGN using recombinant hDC-SIGN Fc. **C.** The frequency of antigen-specific $CD8^+$ T cells after prime (day 7 blood) and boost (day 21 spleen) injections is higher in mice vaccinated with Lewis Y-modified AMAX compared to unmodified AMAX. **D.** Peptide re-stimulation of splenocytes from vaccinated mice show enhanced cytokine-producing $CD8^+$ T cells and $CD4^+$ T cells using with Lewis Y-modified AMAX compared to unmodified AMAX. **E.** Using single injection prime vaccination, AddaVax shows synergistic augmentation of AMAX:Lewis/αCD40 vaccines compared to PBS or the TLR4-stimulus monophosphoryl lipid A (MPLA). **F.** Peptide restimulation of splenocytes from vaccinated mice shows comparable increases in IFNγ-producing $CD8^+$ T cells by AddaVax. $CD4^+$ T cell activation after peptide restimulation was also boosted, although this was similar to MPLA. **G.** Unsupervised clustering of antigen-specific $CD44^+CD62L^-CD8^+$ T cells by tSNE using CD127, KLRG1 and CXCR3 shows significant different phenotypes of T cells induced by different adjuvants. **H.** Quantification shows a significant enrichment of $KLRG1^{high}$ $CD8^+$ T cells in the vaccination group containing AddaVax. ELISA data (mean + -SEM of experimental triplicate) representative of at least 2 different batches of product. *In vivo* data (mean ± SEM) representative of 2 independent experiments with group size N = 10 for C/D and N = 5 for G-H. Statistics by one-way ANOVA with Tukey post-hoc multiple comparison test, D,F statistics on total %cytokine-producing cells; $*p < 0.05$ $**p < 0.01$ $***p < 0.001$ $****p < 0.0001$.

potent antigen-specific $CD8^+$ and $CD4^+$ T cell immune response can be elicited.

3.7. *Incorporation of tumor-associated self-antigens into AMAX leads to increased de novo $CD8^+$ and $CD4^+$ T cell responses*

Finally, we investigated the efficacy of AMAX to induce antigen-specific $CD8^+$ T cell responses to tumor-associated self-antigens like GP100, TRP1 and TRP2[28–30]. We generated synthetic long peptides and AMAX harboring the $CD8^+$ T cell-reactive GP100 epitope and the pan HLA-DR (PADRE) $CD4^+$ T cell-reactive epitope [31]. A single injection of GP100-PADRE AMAX with the AddaVax/αCD40 adjuvant combination induced *de novo* antigen-specific $CD8^+$ T cell responses to the GP100 epitope as measured using GP100-H2-kb tetramers (Fig. 7A). Peptide

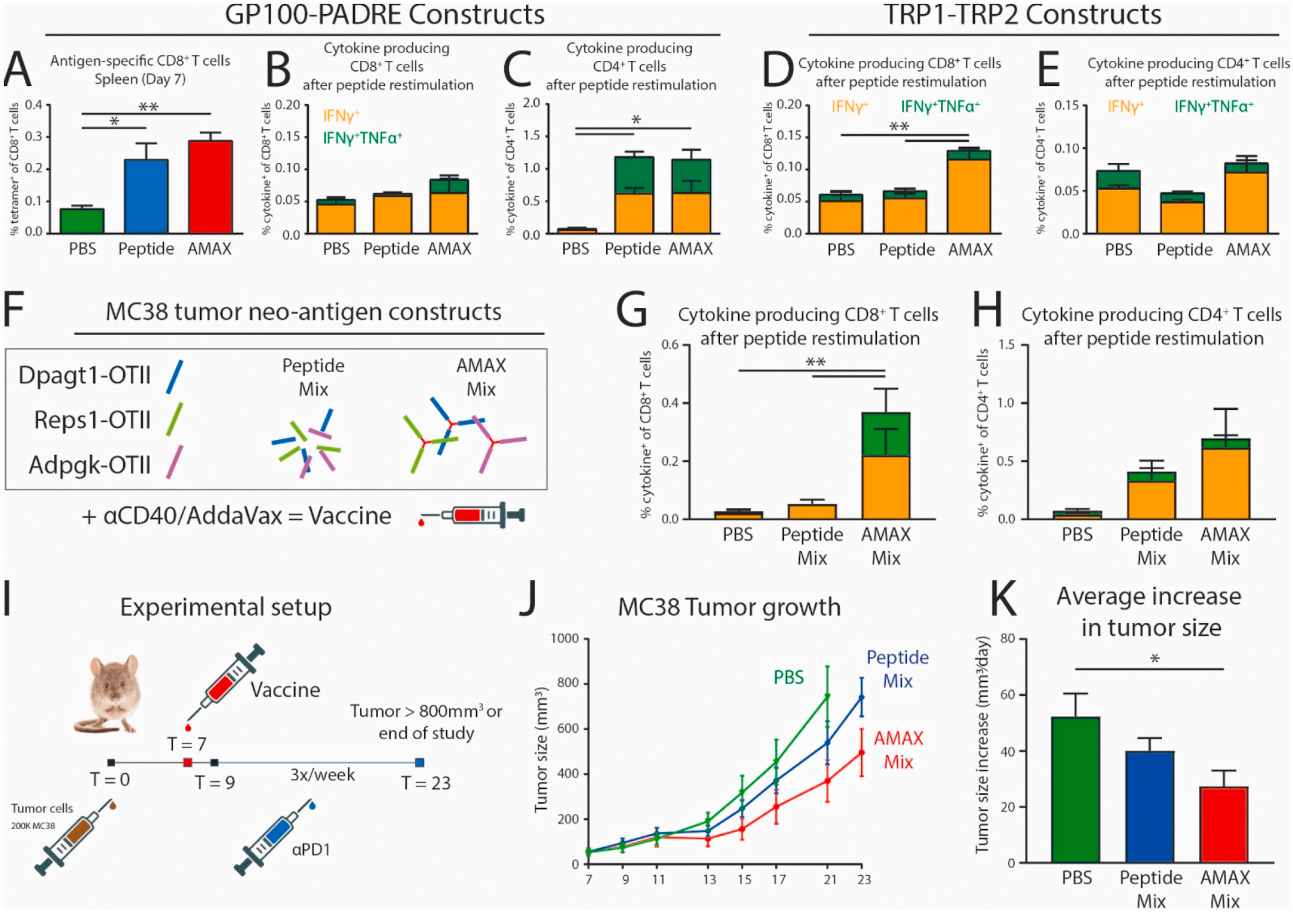

Fig. 7. | Tumor-specific AMAX immunization enhances anti-tumor immunity A. GP100-PADRE constructed AMAX with agonistic CD40 and AddaVax induces antigen-specific $CD8^+$ T cells after a single s.c. vaccination. **B–C.** Peptide re-stimulation of splenocytes from vaccinated mice reveal low, but detectable levels of GP100-specific $CD8^+$ T cells (**B.**) and PADRE-specific $CD4^+$ T cells (**C.**). TRP1-TRP2 constructed AMAX induced antigen-specific $CD8^+$ and $CD4^+$ T cells as evidenced by cytokine-producing $CD8^+$ (**D.**) and $CD4^+$ T cells (**E.**) after peptide re-stimulation. **F.** CD8-reactive neoantigens from the MC38 murine colorectal carcinoma were synthesized as peptides and AMAX, including the OTII CD4 epitope. **G.** Percentage cytokine-producing $CD8^+$ T cells after peptide restimulation after mice subcutaneously immunized with the peptide or AMAX mix, in combination with agonistic CD40/AddaVax. **H.** Percentage cytokine producing $CD4^+$ T cells after peptide restimulation. **I.** Mice were subcutaneously inoculated with MC38 tumor cells. 7 days after tumor cells injection, mice were immunized with PBS, peptide mix or AMAX mix containing neoantigens. 2 days later, antagonistic PD1 therapy started three times a week until end of study. **J.** Experimental groups were divided and tumor growth measured starting with moment of immunization (T = 7). **K.** Quantification of the growth curve (average increase in tumor size) per individual tumor/mouse shows significantly decreased tumor growth in the immunized groups. A–E: Data (mean ± SEM) is representative of two independent experiments with group size N = 9/10. G/H: Data (mean ± SEM) with a group size of N = 8. J/K: Combined data (mean ± SEM) from two independent experiments with group size N = 10–12. Statistics by one-way ANOVA with Tukey post-hoc multiple comparison test, B-E and G,H statistics on total %cytokine-producing cells; *$p < 0.05$ **$p < 0.01$ ***$p < 0.001$ ****$p < 0.0001$.

re-stimulation combined with intracellular cytokine staining was less sensitive, but a similar trend was evident (Fig. 7B). Although no difference in numbers was observed between the peptide and AMAX vaccinated condition, PADRE-specific $CD4^+$ T cells were also efficiently induced (Fig. 7C). Next, we explored peptidic constructs containing the melanoma-associated TRP1 $CD8^+$ T cell-reactive and TRP2 $CD4^+$ T cell-reactive epitope. Since we did not possess TRP1 or TRP2 detecting tetramers, vaccination efficacy with these products was measured using peptide restimulation and intracellular cytokine staining. With these constructs, only AMAX induced TRP1-specific $CD8^+$ T cell responses (Fig. 7D), as well as, $CD4^+$ T cell responses (Fig. 7E).

The prevalence of somatic mutations among human cancers has been shown to drive immunogenicity due to the presence of mutated "non-self" antigens, called neoantigens [9]. These patient-specific neo--antigens are increasingly being identified and used as anti-tumor vaccine component [10,32]. As such, we synthesized peptides and AMAX versions of previously identified neoantigens specific for MC38 mouse tumor cells [9] (Fig. 7F). By combining the CD8 T cell-specific MC38 neoantigens with the OTII CD4 T cell-specific antigen, we could test the universality of the AMAX platform in a vaccination and anti-tumor setting. The AMAX platform induced significantly higher frequencies of neoantigen-specific $CD8^+$ T cells after a single prime immunization (Fig. 7G). Also, the frequency of OTII-specific $CD4^+$ T cells increased, although this was not statistically significant. Finally, to investigate the anti-tumor capacity of the AMAX platform, we designed a clinically relevant setting of anti-tumor vaccination which includes a regiment of PD1 immune checkpoint blockade (ICB; Fig. 7I). First, mice were subcutaneously inoculated with MC38 tumor cells for 7 days, after which palpable tumors were established and mice were immunized with PBS, the mix of peptides or the mix of AMAX constructs. Two days later, PD1 ICB was started three times per week in all groups. Interestingly, six days after the immunization (T = 13) the effect of neo-antigen immunization became apparent, which continued until the end of the study (Fig. 7J). Importantly, the immunization with the AMAX neoantigen constructs significantly reduced tumor growth in this setting (Fig. 7K).

4. Discussion

We have shown that formulating a peptide vaccine into a multivalent trimer containing $CD8^+$ T cell epitopes and $CD4^+$ T cell epitopes can induce antigen-specific $CD8^+$ and $CD4^+$ T cell activation *in vitro* and *in vivo*. In a classical prime-boost vaccination strategy, trimers outperformed single peptides in terms of antigen-specific $CD8^+$ T cell frequency, cytokine production after peptide restimulation and effector phenotype. As a result, recognition of tumor cells expression the cognate antigen by $CD8^+$ T cells isolated from mice vaccinated with trimers, resulted in IFNγ production and tumor cell death. In our attempt to synthesize several other trimers using solid phase synthesis with changes in hydrophobicity, we noticed poor yield and difficulty to purify the trimers. Linear synthetic peptides are generally synthesized by Fmoc chemistry, based on sequential addition of amino acids to extend the product. This was mainly due to the increased length of the complex trimer. The length of the synthetic peptide is limited by several factors, including the reaction yield or aggregation-prone sequences [23]. As a result, reagents are lost and the more side products are generated, the more troublesome it becomes to purify the target product by high-performance liquid chromatography (HPLC). To overcome this inefficient production, we have developed a chemical nanoplatform that facilitates highly efficient conjugation of pure pre-synthesized peptides, resulting in a product termed Antigen MAtriX (AMAX). This procedure facilitates production of trimers with high yield and purity, while maintaining the trimeric structure and increased immunogenicity. It additionally maximizes the applicability of peptidic constructs in the clinic [23].

In terms of therapeutic effect, vaccination of mice with AMAX combined with anti-CD40 increased the frequency of antigen-specific $CD8^+$ T cells. Since the discovery that ligation of the CD40 receptor on antigen presenting cells boosts the priming of CD8 T cells [33,34], agonistic CD40 antibody has been shown a potent adjuvant in several peptide vaccines [24,35,36]. Importantly, the use of agonistic CD40 antibody has now been shown to mediate potent anti-tumor immunity without active vaccination [37–40], especially in combination with checkpoint inhibitors like antagonistic PD1 antibody [41]. This provides additional rationale to combine peptide vaccination with agonistic CD40 antibody as a therapeutic strategy against tumors. In the current study, we sought to improve the cellular response induced by anti-CD40/AMAX vaccination through a combination with well characterized and clinically-approved adjuvants. MF59 (AddaVax) is a clinically approved squalene oil-in-water adjuvants used in seasonal influenza vaccines for over 20 years [42,43]. Surprisingly, AMAX did not induce antigen-specific $CD8^+$ T cells when combined with AddaVax alone. However, both $CD4^+$ and $CD8^+$ T cell responses were synergistically boosted to high frequency by the combination of anti-CD40 and AddaVax. It is known MF59 induces the formation of germinal center responses and consecutive high affinity antibody production by B cells [44,45]. However, the augmentation of both $CD8^+$ and $CD4^+$ T cell responses by AddaVax in combination with anti-CD40 is a completely novel finding. Not only does this combination increase the frequency of antigen-specific T cells, it also highly promotes the differentiation to antigen-specific $CD62L^{low}KLRG1^{high}$ $CD8^+$ T cells. This phenotype of $CD8^+$ T cell has been suggested to represent terminally differentiated effector T cells responsible for protective immunity [46,47]. This functional effective phenotype of $CD8^+$ T cells is suggested by the therapeutic anti-tumor experiments, although tumor rejection was not complete. The functional distinction between terminal differentiation and plasticity of $CD8^+$ T cells is currently hotly debated and unclear [48]. By unbiased analysis we have described the differences in phenotypes of vaccine-generated antigen-specific $CD8^+$ T cells, which show a surprising susceptibility to adjuvant selection. Two independent studies have shown that $CD62L^-$ effector $CD8^+$ T cells expressing high levels of KLRG1 can dedifferentiate into memory T cells capable of long-term protective immunity [49,50]. How adjuvant selection and AMAX vaccination affects the spatiotemporal distinction between effector and memory function or quantity and quality is beyond the scope of the current study, but an interesting challenge to address in future studies.

How AddaVax specifically augments the αCD40/AMAX vaccine remains to be defined. Since KLRG1 expression on $CD8^+$ T cells is regulated by T-bet upon antigen recognition and IL-12 production [51], it is likely the phenotype induced by AddaVax is influenced by dendritic cells. Several findings might implicate monocyte-derived dendritic cells (moDCs) in this observation. First, MF59 has been shown to promote the attraction and differentiation of monocytes to moDCs [52–54]. Secondly, the *in vivo* efficacy of MF59 depends on the intact MyD88 signaling [55] and moDCs can become the main IL-12 producers under inflammatory conditions in a MyD88-dependent manner [56]. Additionally, DC-SIGN has been often used as the primary marker for moDCs [57,58] and effectively targeted in this study and others [59–61]. However, it remains to defined specifically how the synergy between agonistic CD40 and MF59 (AddaVax) is orchestrated.

Since professional antigen presenting cells like dendritic cells are key in initiating adaptive immunity, targeting antigens to dendritic cells has been proposed as a viable vaccination strategy [62–64]. Dendritic cells express several pattern recognition receptors that are inherently capable of binding foreign antigen and facilitating uptake and antigen presentation to T cells [62]. DC-SIGN (Dendritic Cell-Specific Intercellular adhesion molecule-3-Grabbing Non-integrin) is one such receptor that facilitates the uptake of glycosylated pathogens by dendritic cells for antigen presentation to T cells [65,66]. By conjugating DC-SIGN-binding glycans to antigens, vaccination efficacy can be increased [61]. As such, we show that targeting Lewis Y-modified AMAX to dendritic cells, the cellular immune response is significantly boosted in hDC-SIGN transgenic mice.

Precise mechanistic insight into the success of trimers over peptides remains to be investigated. In our *in vitro* studies using BMDCs or splenic $CD11c^+$ DCs, we could not discern a significant benefit of trimers over peptides. This suggests that the enhanced immunogenicity of AMAX constructs is dependent on the *in vivo* setting and possibly does not involve the construct-DC interface, but instead bioavailability at the injection site or in the draining lymph node. Also, differences between larger particulate antigens and soluble have been suggested to critically affect immunogenicity in vaccines [67]. Both synthetic long peptide of approx. 3500kD and [28.]' [29.]' [30.] AMAX products of 12000kD are soluble and do not form visual aggregates in our hands, regardless of the incorporated antigenic peptide sequence. Also, the surface charge or zeta potential of drug delivery systems have been shown to affect the biological availability and *in vivo* mode of action [68]. However, the different AMAX products comprise different amino acid sequences and therefore different zeta potentials. Regardless of these differences in charge, the AMAX outperformed single peptides in terms of cellular immunity, suggesting the zeta potential is of minor consequence in our immunization strategies. Hence, the functional difference in mechanism of action between peptide and AMAX occur *in vivo* on a molecular scale that warrants further investigation.

As our understanding of the immune system increases, the approach to rational vaccine design changes. In an era where technological advancements are increasing the potential of precision medicine, the possibility of antigen discovery, synthesis of highly defined peptidic vaccines and need for T cell-mediated vaccines are tied together. Since the revolution of immunotherapeutic in cancer, the interest for dendritic cell-mediated immune responses have spiked. Therefore, clearly defined improvements of peptide-based vaccination strategies aimed at using dendritic cells *in situ* are of increasing importance. Importantly, we show the incorporation of neoantigen, as well as tumor-associated antigens, into AMAX constructs capable of inducing *de novo* T cell responses. Importantly, therapeutic immunization with neoantigen AMAX constructs reinforced PD1 ICB in a syngeneic mouse tumor model. In a therapeutic clinical setting, neo-antigen-containing AMAX vaccination

may complement existing immune responses that can be unleashed by antagonistic PD1 antibody with *de novo* generated immune responses by AMAX. Also, in none of the *in vivo* experiments did we encounter unwarranted internal or external pathological side effects, suggesting a favorable safety profile. In summary, we provide a clearly defined peptide-based vaccination strategy capable of generating high quality $CD8^+$ and $CD4^+$ T cell responses for immunotherapeutic purposes.

CRediT author contribution statement

Sjoerd T.T. Schetters: Conceptualization, Methodology, Performed and analyzed experiments, Writing - original draft. **R.J. Eveline Li:** synthesized the products, Writing - original draft. **Laura J.W. Kruijssen:** Performed and analyzed experiments. **Steef Engels:** Performed and analyzed experiments. **Martino Ambrosini:** synthesized the products. **Juan J. Garcia-Vallejo:** Methodology. **Hakan Kalay:** Conceptualization, synthesized the products. **Wendy W.J. Unger:** Conceptualization, Methodology, Writing - original draft. **Yvette van Kooyk:** Conceptualization, Methodology, Writing - original draft, Supervision.

Declaration of competing interest

The authors declare that they have no known competing financial interests or personal relationships that could have appeared to influence the work reported in this paper.

Acknowledgements

The authors would like to thank Tanja Konijn and Tom O'Toole for excellent flow cytometry support at the O2Flow, Amsterdam UMC, The Netherlands. We would like to thank dr. Louis Boon from Polpharma Biologics for providing the antagonistic PD1 antibody.

Appendix A. Supplementary data

Supplementary data to this article can be found online at https://doi.org/10.1016/j.biomaterials.2020.120342.

S.T.T.S., R.J.E.L., L.K., S.E., J.G-V., W.W.J.U., Y.K. are supported by the European Research Council (ERC-339977-Glycotreat).

The raw/processed data required to reproduce these findings cannot be shared at this time due to technical or time limitations. However, the corresponding authors are open to any inquiries regarding the data published in this manuscript.

References

[1] L.H. Jones, Recent advances in the molecular design of synthetic vaccines, Nat. Chem. 7 (2015) 952.
[2] J.P. Tam, Recent advances in multiple antigen peptides, J. Immunol. Methods 196 (1996) 17–32.
[3] W. Li, M.D. Joshi, S. Singhania, K.H. Ramsey, A.K. Murthy, Peptide vaccine: progress and challenges, Vaccines 2 (2014) 515–536.
[4] W.C. Koff, et al., Accelerating next-generation vaccine development for global disease prevention, Science 340 (80) (2013).
[5] A. Sette, R. Rappuoli, Reverse vaccinology: developing vaccines in the era of genomics, Immunity 33 (2010) 530–541.
[6] V. Dutoit, et al., Exploiting the glioblastoma peptidome to discover novel tumour-associated antigens for immunotherapy, Brain 135 (2012) 1042–1054.
[7] R. Rampling, et al., A cancer Research UK first time in human phase I trial of IMA950 (novel multipeptide therapeutic vaccine) in patients with newly diagnosed glioblastoma, Clin. Canc. Res. 22 (2016) 4776–4785.
[8] V. Dutoit, et al., Antigenic expression and spontaneous immune responses support the use of a selected peptide set from the IMA950 glioblastoma vaccine for immunotherapy of grade II and III glioma, OncoImmunology 7 (2018), e1391972.
[9] M. Yadav, et al., Predicting immunogenic tumour mutations by combining mass spectrometry and exome sequencing, Nature 515 (2014) 572.
[10] P.A. Ott, et al., An immunogenic personal neoantigen vaccine for patients with melanoma, Nature 547 (2017) 217.
[11] O. Takeuchi, S. Akira, Pattern recognition receptors and inflammation, Cell 140 (2010) 805–820.
[12] R.L. Coffman, A. Sher, R.A. Seder, Vaccine adjuvants: putting innate immunity to work, Immunity 33 (2010) 492–503.
[13] B. Hou, B. Reizis, A.L. DeFranco, Toll-like receptors activate innate and adaptive immunity by using dendritic cell-intrinsic and -extrinsic mechanisms, Immunity 29 (2008) 272–282.
[14] Y. Hailemichael, et al., Persistent antigen at vaccination sites induces tumor-specific CD8+ T cell sequestration, dysfunction and deletion, Nat. Med. 19 (2013) 465.
[15] S. Rosendahl Huber, J. van Beek, J. de Jonge, W. Luytjes, D.T. van Baarle, Cell responses to viral infections – opportunities for peptide vaccination, Front. Immunol. 5 (2014) 171.
[16] O. Kepp, et al., Trial watch: peptide-based vaccines in anticancer therapy AU - Bezu, Lucillia, OncoImmunology 7 (2018), e1511506.
[17] I. Melero, et al., Therapeutic vaccines for cancer: an overview of clinical trials, Nat. Rev. Clin. Oncol. 11 (2014) 509.
[18] M. Schaefer, et al., Decreased pathology and prolonged survival of human DC-SIGN transgenic mice during mycobacterial infection, J. Immunol. 180 (2008) 6836–6845.
[19] K.A. Hogquist, et al., T cell receptor antagonist peptides induce positive selection, Cell 76 (1994) 17–27.
[20] M.J. Barnden, J. Allison, W.R. Heath, F.R. Carbone, Defective TCR expression in transgenic mice constructed using cDNA-based [agr]- and [bgr]-chain genes under the control of heterologous regulatory elements, Immunol. Cell Biol. 76 (1998) 34–40.
[21] M.B. Lutz, et al., An advanced culture method for generating large quantities of highly pure dendritic cells from mouse bone marrow, J. Immunol. Methods 223 (1999) 77–92.
[22] S.H. van der Burg, R. Arens, F. Ossendorp, T. van Hall, C.J.M. Melief, Vaccines for established cancer: overcoming the challenges posed by immune evasion, Nat. Rev. Canc. 16 (2016) 219.
[23] P. Vlieghe, V. Lisowski, J. Martinez, M. Khrestchatisky, Synthetic therapeutic peptides: science and market, Drug Discov. Today 15 (2010) 40–56.
[24] M.S. Rolph, S.H.E. Kaufmann, CD40 signaling converts a minimally immunogenic antigen into a potent vaccine against the intracellular pathogen Listeria monocytogenes, J. Immunol. 166 (2001) 5115–5121.
[25] H.-I. Cho, E. Celis, Optimized peptide vaccines eliciting extensive CD8 T-cell responses with therapeutic antitumor effects, Canc. Res. 69 (2009) 9012–9019.
[26] K. Palucka, J. Banchereau, I. Mellman, Designing vaccines based on Biology of human dendritic cell subsets, Immunity 33 (2010) 464–478.
[27] C.M. Fehres, et al., Cross-presentation through langerin and DC-SIGN targeting requires different formulations of glycan-modified antigens, J. Contr. Release 203 (2015) 67–76.
[28] W.W. Overwijk, et al., gp100/pmel 17 is a murine tumor rejection antigen: induction of 'self'-reactive, tumoricidal T cells using high-affinity, altered peptide ligand, J. Exp. Med. 188 (1998) 277–286.
[29] S.K. Mendiratta, et al., Therapeutic tumor immunity induced by polyimmunization with melanoma antigens gp100 and TRP-2, Canc. Res. 61 (2001) 859–863.
[30] R.-F. Wang, E. Appella, Y. Kawakami, X. Kang, S.A. Rosenberg, Identification of TRP-2 as a human tumor antigen recognized by cytotoxic T lymphocytes, J. Exp. Med. 184 (1996) 2207–2216.
[31] J. Alexander, et al., Development of high potency universal DR-restricted helper epitopes by modification of high affinity DR-blocking peptides, Immunity 1 (1994) 751–761.
[32] J.C. Castle, et al., Exploiting the mutanome for tumor vaccination, Canc. Res. 72 (2012) 1081–1091.
[33] S.P. Schoenberger, R.E.M. Toes, E.I.H. van der Voort, R. Offringa, C.J.M. Melief, T-cell help for cytotoxic T lymphocytes is mediated by CD40–CD40L interactions, Nature 393 (1998) 480.
[34] M. Cella, et al., Ligation of CD40 on dendritic cells triggers production of high levels of interleukin-12 and enhances T cell stimulatory capacity: T-T help via APC activation, J. Exp. Med. 184 (1996) 747–752.
[35] D. Ito, K. Ogasawara, K. Iwabuchi, Y. Inuyama, K. Onoé, Induction of CTL responses by simultaneous administration of liposomal peptide vaccine with anti-CD40 and anti-CTLA-4 mAb, J. Immunol. 164 (2000) 1230–1235.
[36] L. Diehl, et al., CD40 activation in vivo overcomes peptide-induced peripheral cytotoxic T-lymphocyte tolerance and augments anti-tumor vaccine efficacy, Nat. Med. 5 (1999) 774.
[37] F. Li, J.V. Ravetch, Inhibitory Fcγ receptor engagement drives adjuvant and anti-tumor activities of agonistic CD40 antibodies, Science 333 (80) (2011) 1030–1034.
[38] G.L. Beatty, et al., CD40 agonists alter tumor stroma and show efficacy against pancreatic carcinoma in mice and humans, Science 331 (80) (2011) 1612–1616.
[39] I. Marigo, et al., T cell cancer therapy requires CD40-CD40L activation of tumor necrosis factor and inducible nitric-oxide-synthase-producing dendritic cells, Canc. Cell 30 (2016) 377–390.
[40] M.F. Fransen, et al., Effectiveness of slow-release systems in CD40 agonistic antibody immunotherapy of cancer, Vaccine 32 (2014) 1654–1660.
[41] C.S. Garris, et al., Successful Anti-PD-1 Cancer Immunotherapy Requires T Cell-Dendritic Cell Crosstalk Involving the Cytokines IFN-γ and IL-12. *Immunity* vol. **49**, 2018, pp. 1148–1161.
[42] T. Derek, O. Hagan, MF59 is a safe and potent vaccine adjuvant that enhances protection against influenza virus infection, Expert Rev. Vaccines 6 (2007) 699–710.
[43] T. Vesikari, et al., Efficacy, immunogenicity, and safety evaluation of an MF59-adjuvanted quadrivalent influenza virus vaccine compared with non-adjuvanted influenza vaccine in children: a multicentre, randomised controlled, observer-blinded, phase 3 trial, Lancet Respir. Med. 6 (2018) 345–356.

[44] B. Mastelic Gavillet, et al., MF59 mediates its B cell adjuvanticity by promoting T follicular helper cells and thus germinal center responses in adult and early life, J. Immunol. 194 (2015) 4836–4845.
[45] S. Khurana, et al., MF59 adjuvant enhances diversity and affinity of antibody-mediated immune response to pandemic influenza vaccines, Sci. Transl. Med. 3 (2011), 85ra48 LP-85ra48.
[46] J.A. Olson, C. McDonald-Hyman, S.C. Jameson, S.E. Hamilton, Effector-like CD8^{+} T cells in the memory population mediate potent protective immunity, Immunity 38 (2013) 1250–1260.
[47] S. Sarkar, et al., Functional and genomic profiling of effector CD8 T cell subsets with distinct memory fates, J. Exp. Med. 205 (2008) 625–640.
[48] E. Lugli, G. Galletti, S.K. Boi, B.A. Youngblood, Stem, effector, and hybrid states of memory CD8+ T cells, Trends Immunol. 41 (2020) 17–28.
[49] B. Youngblood, et al., Effector CD8 T cells dedifferentiate into long-lived memory cells, Nature 552 (2017) 404–409.
[50] D. Herndler-Brandstetter, et al., KLRG1+ effector CD8+ T cells lose KLRG1, differentiate into all memory T cell lineages, and convey enhanced protective immunity, Immunity 48 (2018) 716–729, e8.
[51] N.S. Joshi, et al., Inflammation directs memory precursor and short-lived effector CD8+ T cell fates via the graded expression of T-bet transcription factor, Immunity 27 (2007) 281–295.
[52] R. Cioncada, et al., Vaccine adjuvant MF59 promotes the intranodal differentiation of antigen-loaded and activated monocyte-derived dendritic cells, PloS One 12 (2017), e0185843.
[53] A. Seubert, E. Monaci, M. Pizza, D.T. O\textquoterightHagan, A. Wack, The adjuvants aluminum hydroxide and MF59 induce monocyte and granulocyte chemoattractants and enhance monocyte differentiation toward dendritic cells, J. Immunol. 180 (2008) 5402–5412.
[54] S.T.T. Schetters, et al., Immunological dynamics after subcutaneous immunization with a squalene-based oil-in-water adjuvant, FASEB J. n/a 34 (9) (2020) 12406–12418.
[55] A. Seubert, et al., Adjuvanticity of the oil-in-water emulsion MF59 is independent of Nlrp3 inflammasome but requires the adaptor protein MyD88, Proc. Natl. Acad. Sci. Unit. States Am. 108 (2011) 11169–11174.
[56] Y. Zhan, et al., Resident and monocyte-derived dendritic cells become dominant IL-12 producers under different conditions and signaling pathways, J. Immunol. 185 (2010) 2125–2133.
[57] S. Menezes, et al., The heterogeneity of Ly6Chi monocytes controls their differentiation into iNOS+ macrophages or monocyte-derived dendritic cells, Immunity 45 (2016) 1205–1218.
[58] C. Cheong, et al., Microbial stimulation fully differentiates monocytes to DC-SIGN/CD209 + dendritic cells for immune T cell areas, Cell 143 (2010) 416–429.
[59] S.T.T. Schetters, et al., Mouse DC-SIGN/CD209a as target for antigen delivery and adaptive immunity, Front. Immunol. 9 (2018).
[60] L.N. Velasquez, et al., Targeting Mycobacterium tuberculosis antigens to dendritic cells via the DC-specific-ICAM3-grabbing-nonintegrin receptor induces strong T-helper 1 immune responses, Front. Immunol. 9 (2018) 471.
[61] Y. van Kooyk, W.W.J. Unger, C.M. Fehres, H. Kalay, J.J. García-Vallejo, Glycan-based DC-SIGN targeting vaccines to enhance antigen cross-presentation, Mol. Immunol. 55 (2013) 143–145.
[62] D.J. Irvine, M.A. Swartz, G.L. Szeto, Engineering synthetic vaccines using cues from natural immunity, Nat. Mater. 12 (2013) 978.
[63] M.D. Joshi, W.J. Unger, G. Storm, Y. van Kooyk, E. Mastrobattista, Targeting tumor antigens to dendritic cells using particulate carriers, J. Contr. Release 161 (2012) 25–37.
[64] W.W.J. Unger, et al., Antigen targeting to dendritic cells combined with transient regulatory T cell inhibition results in long-term tumor regression, OncoImmunology 4 (2015), e970462.
[65] T.B.H. Geijtenbeek, -SIGN, A dendritic cell–specific HIV-1-Binding protein that enhances trans-infection of T cells, Cell 100 (2000) 587–597.
[66] A. Engering, et al., The dendritic cell-specific adhesion receptor DC-SIGN internalizes antigen for presentation to T cells, J. Immunol. 168 (2002) 2118–2126.
[67] C.M. Snapper, Distinct immunologic properties of soluble versus particulate antigens, Front. Immunol. 9 (2018) 598.
[68] S. Bhattacharjee, DLS and zeta potential – what they are and what they are not? J. Contr. Release 235 (2016) 337–351.